Synthesis and Photophysical Investigation of New Porphyrin Derivatives with β-Pyrrole Ethynyl Linkage and Corresponding Dyad with [60] Fullerene

Angelo Lembo,[†] Pietro Tagliatesta,*,[†] and Dirk M. Guldi*,[‡]

Institute for Physical Chemistry, Friedrich-Alexander University Erlangen-Nürberg, Egerlandstrasse 3, 91058 Erlangen, Germany, and Dipartimento di Scienze e Tecnologie Chimiche, University of Rome-Tor Vergata, Via della Ricerca Scientifica, 00133 Rome, Italy

Received: May 4, 2006; In Final Form: July 13, 2006

Two new β-substituted arylethynyl *meso*-tetraphenylporphyrins, 2-[(4′-formyl)phenyl]ethynyl-5,10,15,20-tetraphenylporphyrin (system A) and 2-[(4′-methyl)phenyl]ethynyl-5,10,15,20-tetraphenylporphyrin (system B) and their zinc derivatives were synthesized by palladium catalysis, using a synthetic approach that affords high yields of the target systems. Comparative ultraviolet−visible (UV−vis), NMR, and cyclic voltammetry studies of such macrocycles reveal the presence of an extensive conjugation between the tetrapyrrolic ring and the linker, through π−π orbital interaction. This interaction was observed in the form of a "push−pull" effect that moves the electronic charge between the porphyrin and the aldehyde group of system A. System B, bearing a methyl group instead of the formyl group, was synthesized in order to evaluate the effect of the substitution on the charge delocalization, which is necessary to corroborate the push−pull mechanism hypothesis. The new porphyrin, system A, was also used as a starting material for the synthesis of new porphyrin−fullerene dyads in which the [60]fullerene is directly linked to the tetrapyrrolic rings by ethynylenephenylene subunits. Fluorescence and transient absorption measurements of the new dyads reveal that ultrafast energy and electron transfer occur, respectively, in nonpolar and polar solvents, with high values of the rate constant. The UV−vis, NMR, and cyclic voltammetry results show that it is possible for both energy and electron transfer between porphyrin and fullerene to take place through the π-bond interaction. Such results evidence that the coupling between the donor and acceptor moieties is strong enough for possible photovoltaic applications.

Introduction

During the last 10 years, porphyrins and fullerenes have been widely used to build different molecular networks[1] able to mimic the natural photosynthetic processes.[2] The main goal of such studies was to understand the structural parameters that govern these phenomena in order to achieve the storing of solar energy and its conversion into chemical potential.[3] In such types of molecules, porphyrins and fullerenes interact by self-assembly[4] or through covalent bonds.[1,5]

The principal effort for obtaining long-lived charge separation has been focused toward the production of multistep electron transfer[6−10] steps along different subunits, that are not strongly electronically coupled. In a great variety of these systems, porphyrins act as light harvesting systems,[11,12] while ferrocene and C_{60}—that are covalently linked to the phenyl groups of a *meso*-tetraphenylporphyrin—constitute the donor and acceptor groups, respectively. Such a covalent arrangement prevents, however, a modification of the electronic properties of porphyrins. Notably, only a few papers are present in the literature that are concerned with the synthesis and photochemical studies of similar structures having a C_{60} directly linked to the tetrapyrrolic ring.[13−17] In most of these papers, pyrrole reduced porphyrins—chlorin[16] or bacteriochlorin derivatives[15]—are used to synthesize C_{60} containing dyads.

Despite the fact that chlorin and bacteriochlorin derivatives generate long-lived charge separated states, they are very difficult to synthesize. Moreover, often natural compounds must be used as the starting material. Therefore, the application of simple synthetic pathways, able to afford new functionalized porphyrin derivatives, emerges as an important aspect of such studies. Here, we wish to report the synthesis of new β-substituted porphyrins, which exhibit interesting photochemical properties.

The possibility to introduce different substituents at the β-pyrrole positions constitutes a potent possibility to modify the photophysical properties of the tetrapyrrolic ring (i.e., to modulate the porphyrin−fullerene electronic interaction) at will.

It appears plausible to obtain, in the new β-subtituted porphyrins and metalloporphyrins, a complete charge delocalization, that is, along the carbon−carbon bond that links the ethynylenephenylene subunit and the tetrapyrrole ring. This is known as the typical push−pull effect of the oligoethynylenephenylene subunit.[18−20] Such electronic communication gives rise to a very fast photoinduced charge separation in the porphyrin−fullerene dyads.

The structures of the systems studied in this work are reported in Figure 1.

Experimental Section

General Methods. ^{1}H NMR spectra were recorded as $CDCl_3$ solutions on a Bruker AM-400 instrument using tetramethylsilane (TMS) as an internal standard. Chemical shifts are given

---

* To whom correspondence should be addressed. E-mail: pietro.tagliatesta@uniroma2.it (P.T.); dirk.guldi@chemie.uni-erlangen.de (D.M.G.).
† University of Rome-Tor Vergata.
‡ University of Erlangen.

New Porphyrin Derivatives

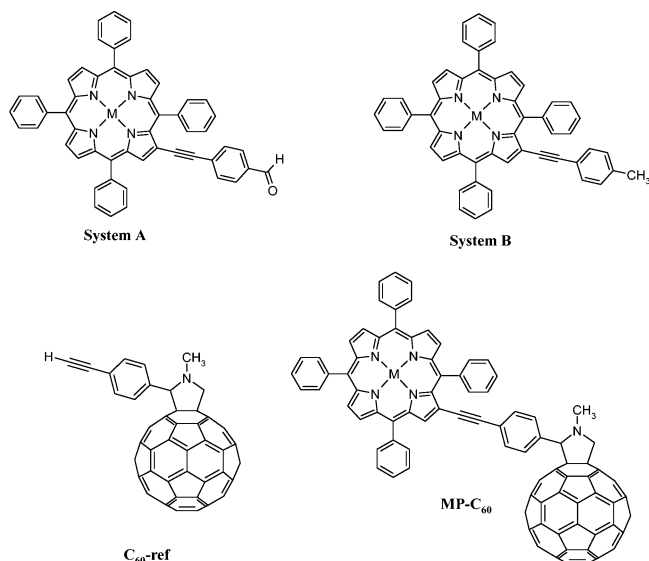*J. Phys. Chem. A, Vol. 110, No. 40, 2006* **11425**

Figure 1. Compounds investigated in this study. M = 2H, Zn.

as δ values. FAB mass spectra were measured on a VG-4 spectrometer using *m*-nitrobenzyl alcohol (NBA) as a matrix. GC mass spectra were recorded on a VG-4 spectrometer equipped with a 30 mt Supelco SPB-5 capillary column. MALDI mass spectra were performed with a MALDI-TOF Reflex IV instrument (Bruker-Daltonics) in reflector mode, using a 337 nm nitrogen laser (8 Hz). A 2 mg/mL 2,5-dihydroxybenzoic acid (gentysic acid) solution in CH_3CN/TFA (0.1% solution) was used as a matrix.

Ultraviolet−visible (UV−vis) spectra were recorded on a Varian Cary 50 Scan spectrophotometer in toluene solution. Steady state fluorescence studies were carried out on a Fluoromax 3 (Horiba) instrument, and all the spectra were corrected for the instrument response. Time resolved fluorescence spectra were recorded on a Photon Technology International Company lifetime spectrofluorometer in the nanosecond time domain with a 337 nm nitrogen laser and elaborated with Felix software. The femtosecond transient absorption studies were performed with 387 nm laser pulses (1 Khz 150 fs pulse width) from an amplified Ti:sapphire laser system (model CPA 2101, Clark-MXR Inc.). Nanosecond laser flash photolysis experiments were performed with 532 nm laser pulses from a Quanta-Ray CDR Nd:YAG system (6 ns pulse width) in a front face geometry. Cyclic voltammetry was carried out with an Autolab electrochemical system, Eco Chemie equipped with PG Stat-12. Current−voltage curves were recorded using GPES, Eco Chemie software. A three-electrode system was used and consisted of a platinum button working electrode, a platinum wire counter electrode, and a saturated calomel reference electrode (SCE). This reference electrode was separated from the bulk of the solution by a fritted-glass bridge filled with a solvent/supporting electrolyte mixture. All potentials are referenced to the SCE.

Chemicals. Silica gel 60 (70−230 and 230−400 mesh, Merck) was used for column chromatography. 1,2-Dichlorobenzene (DCB) for electrochemistry was purchased from Aldrich Chemical Co. and purified by several washings with concentrated H_2SO_4 and distilled over P_2O_5 under vacuum prior to use. Tetra-*n*-butylammonium hexafluorophosphate (TBAPF$_6$), from Aldrich Chemical Co., was recrystallized from ethyl acetate and dried under vacuum at 40 °C for at least 1 week prior to use. High-purity-grade nitrogen gas was purchased from Rivoira. C_{60} was purchased from Term-USA. All other reagents and solvents were from Fluka Chem. Co., Aldrich Chem. Co., or Carlo Erba and were used as received.

Synthesis. *4-(Trimethylsilyl)ethynylbenzaldehyde.*[21] A 16 g (86 mmol) portion of 4-bromobenzaldehyde and 14 g (142 mmol) of trimethylsilylacetylene were dissolved in 100 mL of dried (KOH) triethylamine. The solution was deareated using argon bubbling for 30 min; after that, 227 mg (1 mmol) of Pd-(OAc)$_2$ and 450 mg (1.7 mmol) of PPh$_3$ were added to the solution. The solution was then refluxed under argon, with vigorous stirring. After 4 h, the crude mixture was cooled and filtered and the solid salts were washed with triethylamine. The organic solution was concentrated under vacuum, diluted with dichloromethane (100 mL), and washed with water (3 × 100 mL). The organic layer was separated, dried over anhydrous Na$_2$SO$_4$, and filtered. The solvent was then evaporated under vacuum. The pale yellow residue was purified by column chromatography on silica gel, eluting with petroleum ether (40−70°)/diethyl ether, 98:2, giving the desired product as white crystals, 10.8 g (62% yield). MS (GC): *m/z* 202 [M$^+$]. ^{1}H NMR (400 MHz, CDCl$_3$): δ (ppm) 10.02 (s, 1H), 7.84 (d, 2H; *J* = 8.2 Hz), 7.63 (d, 2H; *J* = 8.2 Hz), 0.29 (s, 9H).

4-Ethynylbenzaldehyde. A 4 g (20 mmol) portion of 4-(trimethylsilyl)ethynylbenzaldehyde was dissolved under nitrogen in 50 mL of CHCl$_3$, and then, a saturated solution (10 mL) of K$_2$CO$_3$ in methanol was added dropwise. After 2 h, water was added to the organic solution. The organic phase was separated, and the aqueous phase was extracted with chloroform. The combined organic solutions were washed with water and dried over anhydrous Na$_2$SO$_4$. The solvent was evaporated under vacuum to give 2.4 g of pure 4-ethynylbenzaldehyde (92% yield). MS (GC): *m/z* 130 [M$^+$]. ^{1}H NMR (400 MHz, CDCl$_3$,): δ (ppm) 9.98 (s, 1H), 7.70 (d, 2H; *J* = 8.2 Hz), 7.50 (d, 2H; *J* = 8.2 Hz), 3.22 (s, 1H).

2-Bromo-5,10,15,20-tetraphenylporphyrin. N-Bromosuccinimide (251 mg, 1.4 mmol) was slowly added to a refluxing solution of *meso*-tetraphenylporphyrin (500 mg, 0.8 mmol) in CHCl$_3$ (150 mL) under nitrogen. After 2 h, the crude mixture was cooled to room temperature and 2 mL of pyridine was added. The solvent was evaporated under vacuum, and the crude product was purified by column chromatography on silica gel, eluting with xylene/petroleum ether (40−70°), 3:2, obtaining 260 mg of the desired porphyrin (yield 46%). MS (FAB): *m/z* 693 [M$^+$], 613 [M − 80]$^+$. ^{1}H NMR (400 MHz, CDCl$_3$): δ (ppm) 8.94−8.91 (br m, 2H), 8.89 (s, 1H), 8.88−8.83 (br m, 2H), 8.79−8.77 (br m, 2H), 8.22 (br m, 6H), 8.11 (br m, 2H), 7.82−7.72 (br m, 12H), −2.82 (br s, 2H).

2-[(4′-Formyl)phenyl]ethynyl-5,10,15,20-tetraphenylporphyrin (System A). A three-neck round-bottom flask, fitted with a condenser, was carefully deoxygenated with a strong stream of dry argon; after that, a solution of 2-bromo-5,10,15,20-tetraphenylporphyrin (260 mg, 0.37 mmol) and 4-ethynylbenzaldehyde (70 mg, 0.54 mmol) in toluene/triethylamine, 5:1 (60 mL), was added. The solution was deareated for 30 min with argon bubbling, and then, Pd(dba)$_2$ (40 mg, 0.07 mmol) and AsPh$_3$ (170 mg, 0.55 mmol) were added. The solution was deareated for a further 5 min; after that, the argon inlet was placed 1 cm above the solution. The argon flow rate was turned up slightly, and the reaction was left under nitrogen at 50 °C. After 16 h, the mixture was cooled at room temperature and the solvent evaporated. The crude product was dissolved in dichloromethane and washed several times with water. The organic solution was dried over anhydrous Na$_2$SO$_4$ and the solvent evaporated under vacuum. The product was purified by column chromatography on silica gel eluting with CH$_2$Cl$_2$/petroleum ether (40−70°), 2:3. The first compound eluted from the column was AsPh$_3$; after that, the polarity of the eluting mixture was gradually increased

11426 *J. Phys. Chem. A, Vol. 110, No. 40, 2006*

Lembo et al.

up to CH_2Cl_2/petroleum ether (40−70°), 3:2. The desired porphyrin obtained from the column was recrystallized from dichloromethane/methanol to give 247 mg of purple powder (yield 90%). MS (FAB): *m/z* 742 [M$^+$]. ^{1}H NMR (400 MHz, CDCl$_3$): δ (ppm) 10.06 (s, 1H), 9.14 (s, 1H), 8.92 (s, 2H), 8.86 (d, 1H; *J* = 5.1 Hz), 8.80 (br s, 3H), 8.25 (br m, 5H), 7.86 (d, 2H; *J* = 8.2 Hz), 7.80−7.66 (br m, 15H), 7.52 (d, 2H; *J* = 8.2 Hz), −2.64 (s, 2H). UV−vis (toluene): λ$_{max}$ (10^{-4}ε) = 432 (20.9), 525 (2.03), 560 (0.62), 602 (0.58), 659 (0.46).

2-[(4′-Methyl)phenyl]ethynyl-5,10,15,20-tetraphenylporphyrin (System B). A solution of 2-bromo-5,10,15,20-tetraphenylporphyrin (40 mg, 57 μmol) and 4-ethynyltoluene (9 mg, 77 μmol) in toluene/triethylamine, 5:1 (36 mL), with Pd(dba)$_2$ (6 mg, 10 μmol) and AsPh$_3$ (24 mg, 80 μmol) was allowed to react under a nitrogen atmosphere for 16 h at 50 °C. The mixture was cooled at room temperature, the solvent evaporated under vacuum, and the residue redissolved in dichloromethane. The organic solution was washed with water (3 × 50 mL), dried over anhydrous Na$_2$SO$_4$, and evaporated under vacuum. The residue was purified on a silica gel column, eluting with CH_2-Cl_2/petroleum ether (40−70°), 25:75, to obtain 33 mg of porphyrin (yield 79%) which was recrystallized from dichloromethane/methanol to give the desired compound as purple powder. MS (FAB): *m/z* 728 [M$^+$]. ^{1}H NMR (400 MHz, CDCl$_3$): δ (ppm) 9.07 (s, 1H), 8.88 (s, 2H), 8.82 (d, 1H; *J* = 5.1 Hz), 8.80 (s, 2H), 8.74 (d, 1H; *J* = 5.1 Hz), 8.23 (br m, 5H), 7.80−7.66 (br m, 15H), 7.25 (d, 2H; *J* = 7.3 Hz), 7.16 (d, 2H; *J* = 7.3 Hz), 2.42 (s, 3H), −2.66 (s, 2H); UV−vis (toluene): λ$_{max}$ (10^{-4}ε) = 428 (22.5), 523 (2.15), 558 (0.609), 600 (0.59), 657 (0.36).

H$_2$P−C$_{60}$. A mixture of 2-[(4′-formyl)phenyl]ethynyl-5,10,-15,20-tetraphenylporphyrin (35 mg, 47 μmol), C$_{60}$ (150 mg, 200 μmol), and *N*-methylglicine (185 mg, 0.2 mmol) was refluxed for 24 h in anhydrous toluene under a nitrogen atmosphere. After cooling, the solvent was evaporated and the residue purified on a silica gel column, eluting with toluene, recovering the unreacted [60]fullerene as the first fraction, the reaction product as the second (42 mg, yield 59%), and the unreacted porphyrin as the third one. MS (FAB): *m/z* 1490 [M + H]$^+$, 769 [M − 720]$^+$, 720 [M − 769]$^+$. ^{1}H NMR (400 MHz, CDCl$_3$): δ (ppm) 9.07 (s, 1H), 8.89 (s, 2H), 8.82 (d, 1H; *J* = 5.1 Hz), 8.79 (s, 2H), 8.73 (d, 1H; *J* = 5.1 Hz), 8.22 (br m, 5H), 7.79 (br m, 15H), 7.61 (br, m, 2H), 7.43 (br, m, 2H), 4.96 (d, 1H; *J* = 9.2 Hz), 4.89 (s, 1H), 4.22 (d, 1H; *J* = 9.2 Hz), 2.86 (s, 3H), −2.68 (s, 2H). UV−vis (toluene): λ$_{max}$ (10^{-4}ε) = 300 (4.88), 429 (21.6), 523 (2.1), 558 (0.71), 601 (0.62), 657 (0.38).

General Procedure for Zinc Insertion. To a solution of starting compound (porphyrins or dyad) in chloroform, a saturated solution of Zn(AcO)$_2$ in methanol was added and the mixture was left to react at room temperature under nitrogen for 2 h. The solvent was evaporated, and the product was purified using a plug of silica gel and eluting with chloroform.

2-[(4′-Formyl)phenyl]ethynyl-5,10,15,20-tetraphenylporphyrin Zn(II), (Zn−System A). Zinc porphyrin was obtained following the general procedures previously described. Yield 95%. MS (FAB): *m/z* 805 [M$^+$]. ^{1}H NMR (400 MHz, CDCl$_3$): δ (ppm) 10.06 (s, 1H), 9.30 (s, 1H), 8.96 (s, 2H), 8.95 (s, 2H), 8.91 (d, 1H; *J* = 5.1 Hz), 8.80 (d, 1H; *J* = 5.1 Hz), 8.25 (br m, 5H), 7.88 (d, 2H; *J* = 8.2 Hz), 7.80−7.66 (br m, 15H), 7.55 (d, 2H; *J* = 8.2 Hz). UV−vis (toluene): λ$_{max}$ (10^{-4}ε) = 311 (2.17), 438 (23.8), 559 (1.86), 596 (0.96).

2-[(4′-methyl)phenyl]ethynyl-5,10,15,20-tetraphenylporphyrin Zn(II), (Zn−System B). Yield: 95%. MS (FAB): *m/z* 791 [M$^+$]. ^{1}H NMR (400 MHz, CDCl$_3$): δ (ppm) 9.24 (s, 1H), 8.95

(s, 2H), 8.93 (s, 2H), 8.90 (d, 1H; *J* = 5.1 Hz), 8.80 (d, 1H; *J* = 5.1 Hz), 8.23 (br m, 5H), 7.78−7.66 (br m, 15H), 7.25 (d, 2H; *J* = 7.3 Hz), 7.16 (d, 2H; *J* = 7.3 Hz), 2.42 (s, 3H). UV−vis (toluene): λ$_{max}$ (10^{-4}ε) = 434 (23.9), 558 (1.75), 592 (0.63).

ZnP−C$_{60}$. Yield: 98%. MS (FAB): *m/z* 1552 [M$^+$], 832 [M − 720]$^+$, 720 [M − 832]$^+$. ^{1}H NMR (400 MHz, CDCl$_3$): δ (ppm) 9.24 (s, 1H,), 8.95 (s, 2H), 8.93 (s, 2H), 8.88 (d, 1H; *J* = 5.1 Hz), 8.77 (d, 1H; *J* = 5.1 Hz), 8.22 (br m, 3H), 8.16 (br d, 2H; *J* = 7.2 Hz), 7.80 (br m, 10H), 7.60 (m, 3H), 7.45−7.40 (br m, 4H), 7.20 (d, 2H; *J* = 7.2 Hz), 4.95 (d, 1H; *J* = 9.2 Hz), 4.85 (s, 1H), 4.20 (d, 1H; *J* = 9.2 Hz), 2.87 (s, 3H). UV−vis (toluene): λ$_{max}$ (10^{-4}ε) = 311 (4.8), 434 (26.1), 558 (1.94), 593 (0.82).

N-Methyl-2-(4′-ethynyl)phenyl-3,4-fulleropyrrolidine, (C$_{60}$-ref.). A mixture of 4-ethynylbenzaldehyde (10 mg, 77 μmol), C$_{60}$ (56 mg, 77 μmol), and *N*-methylglicine (54 mg, 0.6 mmol) was refluxed for 24 h in anhydrous toluene under a nitrogen atmosphere. After cooling to room temperature, the solvent was evaporated under vacuum and the residue was purified on a silica gel column, eluting with toluene/petroleum ether (40−70°), 3:2, recovering as the first band the unreacted [60]fullerene, followed by the reaction product (29 mg, yield 42%). MS (MALDI): *m/z* 877 [M$^+$], 720 [M − 157]$^+$. ^{1}H NMR (400 MHz, CDCl$_3$): δ (ppm) 7.81 (d, 2H; *J* = 7.9 Hz), 7.58 (d, 2H; *J* = 7.9 Hz), 5.0 (d, 1H; *J* = 8.9 Hz), 4.96 (s, 1H), 4.28 (d, 1H; *J* = 9.9 Hz), 3.11 (s, 1H), 2.82 (s, 3H). UV−vis (toluene): λ$_{max}$ (10^{-4}ε) = 330 (5.0).

Results and Discussion

Synthesis. We report in Scheme 1 the synthetic pathways for obtaining the porphyrin derivatives. The bromination of *meso*-tetraphenylporphyrin was carried out using *N*-bromosuccinimide as the brominating agent, slightly modifying the literature procedures[22] to obtain a higher yield of the mono-brominated derivative. The two following cross-coupling reactions between the halogenated porphyrin and the two different substituted ethynylbenzenes, 4-ethynylbenzaldehyde for system A and 4-ethynyltoluene for system B, were carried out using the catalytic system Pd(dba)$_2$/AsPh$_3$, developed by Lindsey.[23] Avoiding the use of copper iodide as a cocatalyst, the homocoupling side reaction between the alkynes was suppressed and high yields of the desired compounds were obtained.

Next, the aldehydic group of system A was used to covalently link the [60]fullerene to the porphyrin by the reaction with *N*-methylglicine in toluene.[24] Zinc insertion for all of the compounds was carried out by adding a saturated methanol solution of Zn(OAc)$_2$ to the porphyrin products dissolved in chloroform.

The fullerene derivative, *N*-methyl-2-(4′-ethynyl)phenyl-3,4-fulleropyrrolidine (C$_{60}$-ref), was synthesized by previously reported procedures.[24] All of the porphyrin compounds, H$_2$P−C$_{60}$, and ZnP−C$_{60}$ were characterized by FAB-MS, MALDI, and ^{1}H NMR spectra.

In particular, the ^{1}H NMR spectra of H$_2$P−C$_{60}$ and ZnP−C$_{60}$ show the presence of the characteristic signals of the *N*-methylpyrrolidine derivatives: one singlet at 2.86 ppm due to the methyl substituent on the nitrogen atom, one singlet at 4.89 ppm due to the hydrogen in position 2 of the pyrrolidinic ring, and two doublets at 4.22 and 4.96 due to the methylene protons.

Cyclic Voltammetry Studies. In Table 1, the potentials of the free bases and the corresponding zinc derivatives of all the compounds are reported. The cyclic voltammograms, in DCB
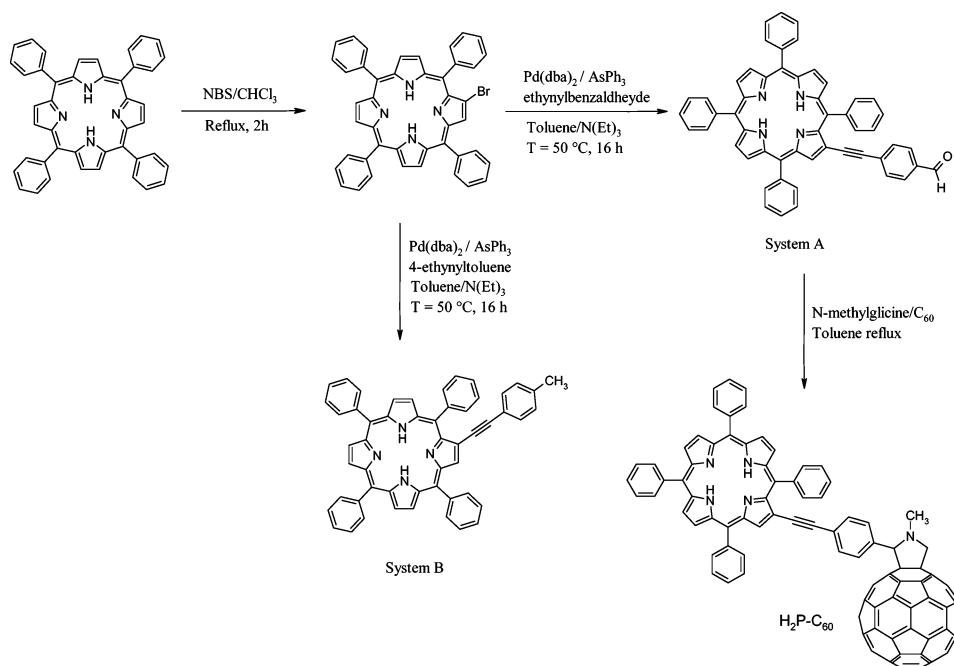
New Porphyrin Derivatives

J. Phys. Chem. A, Vol. 110, No. 40, 2006 **11427**

SCHEME 1: Synthetic Pathways for System A, System B, and H$_2$P−C$_{60}$

TABLE 1: Half-Wave Potentials (V vs SCE) for Reduction and Oxidation of Different Compounds, in DCB Containing 0.05 M TBAPF$_6$

compound	oxidation		reduction			
	VI	V	I	II	III	IV
C$_{60}$-ref		1.55[a]	−0.68	−1.08	−1.68	
H$_2$−TPP	1.48	1.05	−1.24	−1.55		
system A	1.43	1.10	−1.10	−1.34		
system B	1.44	1.08	−1.16	−1.44		
H$_2$P−C$_{60}$	1.43	1.08	−0.66	−1.11	−1.44	−1.67
Zn−TPP	1.25	0.91	−1.45			
Zn−system A	1.21	0.95	−1.28			
Zn−system B	1.17	0.93	−1.33			
ZnP−C$_{60}$	1.19	0.94	−0.66	−1.05	−1.32	−1.57

[a] Irreversible.

(solvent) and with TBAPF$_6$ (supporting electrolyte), reveal the influence of the β-substituent on the oxidation potentials of the porphyrins. In fact, the free base porphyrins of system A and system B are characterized by two reversible oxidation processes centered at 1.10, 1.43 and 1.08, 1.44 V, respectively, while in general H$_2$−TPP shows two reversible oxidations at 1.05 and 1.48 V.[25]

The two systems also present two reversible reductions centered at −1.10 and −1.34 V for system A and −1.16 and −1.44 V for system B. The difference of 60 and 100 mV, respectively, for the first and second reduction potentials between the two systems reflects the electron-withdrawing effect[26] of the aldehydic group of system A. The zinc derivatives of both systems show two reversible oxidations at 0.95 and 1.21 V for system A and 0.93 and 1.17 V for system B, while it is possible to detect only one reversible reduction for both of the compounds at −1.28 and −1.33, respectively.

Figure 2 illustrates the room-temperature cyclic voltammograms of system B, H$_2$P−C$_{60}$, and C$_{60}$-ref in DCB, 0.05 M TBAPF$_6$. H$_2$P−C$_{60}$ undergoes three reversible one-electron and one reversible two-electron reductions and two reversible one-electron oxidations between +1.50 and −2.00 V. The reductions of the H$_2$P−C$_{60}$ occur at $E_{1/2}$ = −0.66, −1.11, −1.44, and −1.67 V. The $E_{1/2}$ values for the second and third reductions are very close to the $E_{1/2}$ values for the first and second reductions of

system B, while the $E_{1/2}$ values for the first and fourth reductions of H$_2$P−C$_{60}$ are almost identical to those for the first and third reductions of C$_{60}$-ref.

The two-electron process centered at −1.11 V derives from the overlapping of two reductions, one from system B and one from C$_{60}$-ref. As shown in Figure 2, the $E_{1/2}$ value for the first and second oxidations of H$_2$P−C$_{60}$ ($E_{1/2}$ = 1.08 and 1.43 V) occur at virtually identical potentials for the first and second oxidations of system B ($E_{1/2}$ = 1.08 and 1.44 V). Such data suggest the porphyrin and fullerene as two different and noninteracting chromophores, retaining their own electronic and physical properties. From the reported data, it is evident that the highest occupied molecular orbital (HOMO)−lowest unoccupied molecular orbital (LUMO) gap of the porphyrin systems
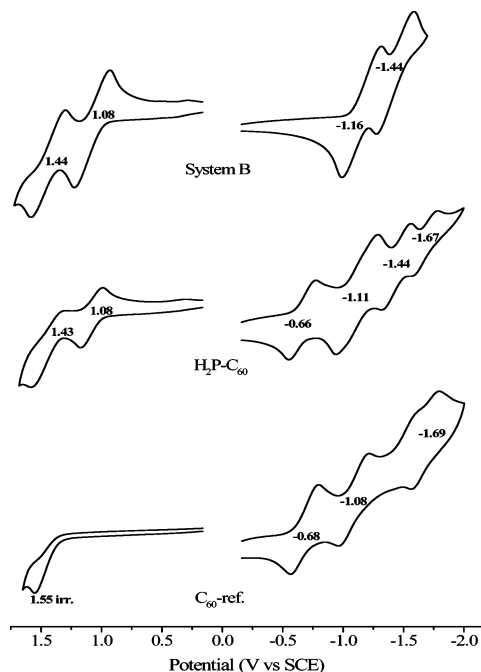

Figure 2. Cyclic voltammograms at 200 mV/s in DCB with 0.05 M TBAPF$_6$ as the supporting electrolyte of system B, H$_2$P−C$_{60}$, and C$_{60}$-ref.

TABLE 2: UV−vis Spectral Data of All the Investigated Compounds in Toluene and THF

	λ_{max} (nm) ($\epsilon 10^{-4}$)	
compound	toluene	THF
system A	311(2.17), 432(20.9), 525(2.03), 560(0.62), 602(0.58), 659(0.46)	428(20.2), 522(1.92), 558(0.59), 601(0.54), 658(0.40)
system B	428(22.5), 523(2.15), 558(0.60), 600(0.59), 657(0.36)	424(20.1), 521(1.89), 556(0.62), 599(0.52), 656(0.32)
H_2P-C_{60}	300(4.88), 429(21.6), 523(2.1), 558(0.71), 601(0.62), 657(0.38)	300(4.6), 425(19.1), 521(1.85), 556(0.65), 600(0.54), 656(0.34)
Zn−system A	311(2.17), 438(23.8), 559(1.86), 596(0.96)	437(22.6), 566(1.72), 603(0.87)
Zn−system B	434(23.9), 558(1.75), 592(0.63)	434(24.7), 564(1.67), 600(0.60)
$ZnP-C_{60}$	311(4.8), 434(26.1), 558(1.94), 593(0.82)	311(4.5), 435(21.6), 565(1.46), 601(0.62)

is lowered going from H_2-TPP, 2.29 V to system B and system A, 2.24 and 2.20 V, respectively. Such an observation is justified by postulating an extension of conjugation along the linker.

By adding the corresponding reduction and oxidation potentials of the electron-accepting C_{60} and electron-donating porphyrins, respectively, we estimate the following radical ion pair energies: H_2P-C_{60}, 1.74 eV; $ZnP-C_{60}$, 1.6 eV.

UV−Visible Studies. The UV−vis spectra of all the compounds show interesting characteristics concerning the porphyrin systems. In Table 2, the spectral features of all the new compounds are reported. The spectra of systems A and B in toluene present a broad Soret band, shifted toward higher wavelengths compared with the Soret band of H_2-TPP.[27] In toluene, the Soret band of system B is located at 428 nm, while that of system A is at 432 nm, with values of the molar extinction coefficients of 2.25×10^5 and 2.09×10^5 M^{-1} cm^{-1}, respectively. H_2P-C_{60} shows the Soret band located at 429 nm, with a molar extinction coefficient of 2.16×10^5 M^{-1} cm^{-1}. Furthermore, in this last spectrum, a broad band, located between 300 and 350 nm, due to the C_{60} moiety is present (Figure 3).

In our opinion, the position of the Soret bands and the ϵ values of such absorptions, compared with those of H_2-TPP, are influenced by the electronic conjugation of the substituents in the β-pyrrole position. The smaller value of ϵ in system A derives from the electron-withdrawing effect of the aldehydic group. The extension of conjugation based on the resonance effect also justifies the shift of the Soret band to higher wavelengths, if compared with the shift of the band of system B. This observation can be justified by the presence of an electron-donating effect of the porphyrin toward the electron-withdrawing aldehydic group of system A, generating a "push−pull" effect that is transmitted through the carbon−carbon skeleton of the ethynylenephenylene subunit. This effect lowers the electron density of the tetrapyrrole ring, in turn lowering the ϵ value of system A. On the contrary, in H_2P-C_{60}, only an

overall electron-withdrawing effect due to the C_{60} moiety can be observed. Furthermore, the Q-bands of all the examined compounds are slightly shifted. The introduction of zinc into the macrocycles produces an increase in the electron density of the rings, giving very similar values of molar extinction coefficients in both porphyrins, 2.38×10^5 and 2.39×10^5 M^{-1} cm^{-1} for systems A and B, respectively, despite the 4 nm difference in the Soret band, 434 nm for system B and 438 nm for system A. The spectra of the free bases and zinc complexes of system B and dyad are virtually superimposable, as illustrated in Figures 3 and 4. From Figure 4, it is also discernible that the $ZnP-C_{60}$ spectrum is the sum of the Zn−system B spectrum and of the *N*-methyl-2-(4′-ethynyl)phenyl-3,4-fulleropyrrolidine compound (C_{60}-ref) which was synthesized as a reference.

NMR Studies. Both porphyrin systems were investigated by ^{1}H NMR spectroscopy. In addition, system A was probed with two different bidimensional NMR methodologies, that is, HSQC and HMBC. HSQC allows mapping of the direct coupling of each proton with its relative bonded carbon atom, and HMBC sheds light onto J^2 and J^3 [1]H−[13]C couplings.[28] These methodologies allowed us to assign the NMR signals concerning the (4′-formyl)phenylethynyl substituent on the pyrrolic ring (Figure 5). From the inspection of the HMBC spectrum of system A, it is possible to see different signals arising from J^2 and J^3 hydrogen−carbon couplings. The two couplings at 135.5 and 129.0 ppm of the aldehydic proton at 10.06 correspond to carbon atoms 2 and 3, respectively.

The most diagnostic signals are those that relate to the ethynylene carbons, which are coupled with protons 4 and 3. Their relative resonance frequencies at 9.14 ppm for proton 4 and 7.52 ppm for proton 3 correspond to the resonance frequency of carbon 7 at 91.0 ppm and carbon 6 at 98.3 ppm.[29] In the HSQC spectrum, it is possible to see five different pyrrolic proton signals coupled with four magnetically different carbon atoms: the first one at 9.14 ppm coupled with the carbon signal
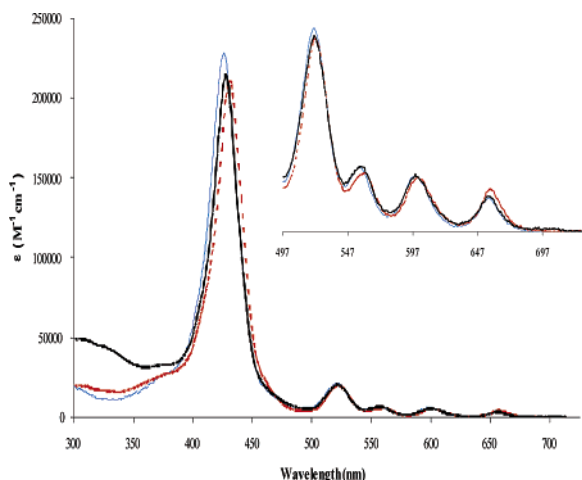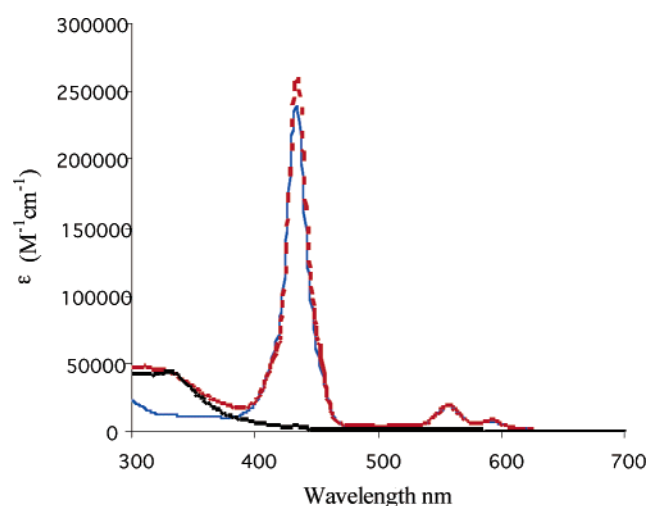

Figure 3. UV−vis spectra of system A (red dotted line), system B (blue solid line), and H_2P-C_{60} (black dashed line). Q-bands are reported in the inset.

Figure 4. UV−vis spectra of $ZnP-C_{60}$ (red line), Zn−system B (blue line), and C_{60}-ref (black line).

New Porphyrin Derivatives

J. Phys. Chem. A, Vol. 110, No. 40, 2006 **11429**
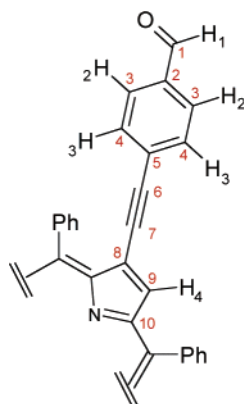

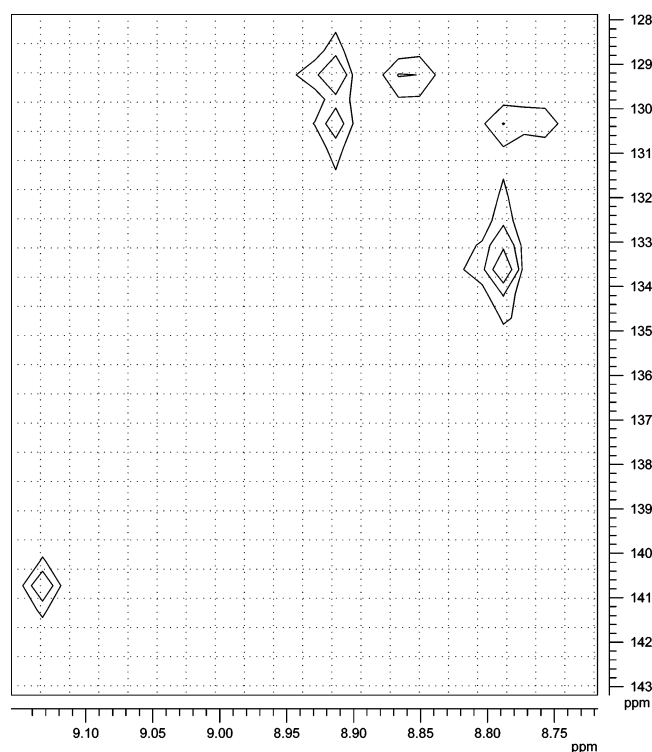**Figure 5.** Carbon and proton assignments of the β-substituent of system A.

Figure 6. HSQC of system A. $^1H-^{13}C$ couplings of β-pyrrolic protons and carbons.

at 141.0 ppm, the second one the singlet at 8.92 ppm, which correspond two different carbon signals at 129.2 and 130.4 ppm, the third one the doublet at 8.87 ppm coupled with a carbon signal at 129.2, then the singlet at 8.80 ppm coupled with a carbon signal at 133.6 ppm, and finally the doublet at 8.80 ppm coupled with the carbon signal at 130.4 ppm (Figure 6).

Comparing the ^1H NMR of system A and system B, it is clear that between 8 and 9 ppm different patterns concerning the pyrrole protons are present (Figure 7). In system B, a doublet at 8.75 ppm is clearly visible, while, in system A, this is superimposed with the singlet at 8.80 ppm. Changing the substituent on the phenyl ring linked to the β-position, a shift toward lower frequencies is evident when going from a methyl to an aldehydic group. Moreover, the NMR shifts do not all have the same magnitude and so the peak at 9.14 ppm in system A (H_1) is shifted in system B to 9.07 ppm (Δppm = 0.07), while all other peaks are shifted by about 0.04 ppm, except the singlet at 8.80 ppm in system A.

It is possible to understand all of these aspects by postulating an extension of the conjugation from the tetrapyrrole ring along

the substituent. Figure 8 depicts the three fundamental resonance structures[30] of porphyrin system A, in which it is clear how only three of the four pyrrolic rings are subjected to the extension of the conjugation. On the other hand, the two protons on the ring C (H_4) are not affected by this charge delocalization and in this case it is possible to attribute these two protons to the singlet at 8.80 ppm in both systems. The β-pyrrole carbon atoms of rings B and D are magnetically equivalent, and we can attribute the carbon signal at 130.4 ppm to the carbon with the positive charge, while the other one corresponds to the signal at 129.2 ppm. Since the resonance effect depends on the distance relative to the aldehydic group, it is possible to visualize the proton H_2 (8.87 ppm) and proton H_3 (8.80 ppm) as doublets. Notably, such an impact is not discernible for the proton H_5 (8.92 ppm), also because the symmetry of porphyrin is lost. The signal at 133.6 ppm is due to the β-pyrrolic carbon atoms of pyrrolic ring C.

These results are in good agreement with the effect of the electron-withdrawing substituents on the β-positions of the tetrapyrrole ring[31] and with the fact that the free base porphryins tend to retain their aromaticity, excluding, however, the two external double bonds. In our case, only one double bond is excluded from the delocalization. Still, in the HSQC spectrum of system B, five different pyrrolic proton signals seem to couple with four magnetically different carbon atoms, but all of the carbon signals are shifted toward higher fields. In particular, while in system A the carbon with the positive charge in the ring A resonates at 141.0 ppm, in system B, such signal is shifted to 138.0 ppm. This constitutes further evidence of the electron-withdrawing effect of the aldehydic group. Finally, it should be noted that the β-pyrrole proton pattern in the ^1H NMR spectrum of the free base dyad is completely similar to that of system B.

The ^1H NMR spectra of the corresponding zinc derivatives present an identical β-pyrrolic proton pattern (Figure 9). In particular, the singlet found at 8.80 ppm for the free base is largely shifted to lower field and this fact is due to the coordination of the zinc atom to the nitrogen atom of the pyrrole ring C. This causes a decrease in electron density on the aforementioned pyrrole ring, and in addition, the average Δppm between pyrrole proton signals of system A and system B is less pronounced in the zinc derivatives relative to the free base porphyrins.

All of the aspects discussed above point to the presence of an extension of conjugation from the porphyrin ring along the β-substituent; especially when an aldehydic group is present on the phenyl ring of the substituent, a push-pull effect takes place from the porphyrin to the aldheyde.

Moreover, since Zn−system A and Zn−system B have more or less the same molar extinction coefficient, it is possible that the zinc atom turns off this phenomenon, because the metal insertion in the tetrapyrrolic ring renders all of the β-pyrrole positions, in terms of resonance structures, equivalent.

Photophysical Studies. In Table 3, the fluorescence properties of all the examined compounds are reported.

Steady state fluorescence spectra were recorded to analyze the photophysical properties of the new porphyrins and dyads. The steady state fluorescence studies were recorded in four different solvents: toluene, chloroform, tetrahydrofuran (THF), and benzonitrile. The excitation wavelength was 525 nm for the free base derivatives and 560 nm for the zinc derivatives. In toluene, system A presents two emission bands at 666 and 734 nm, while system B, at 663 and 731 nm. Such a difference of 3 nm remains also in the other solvents. In the corresponding
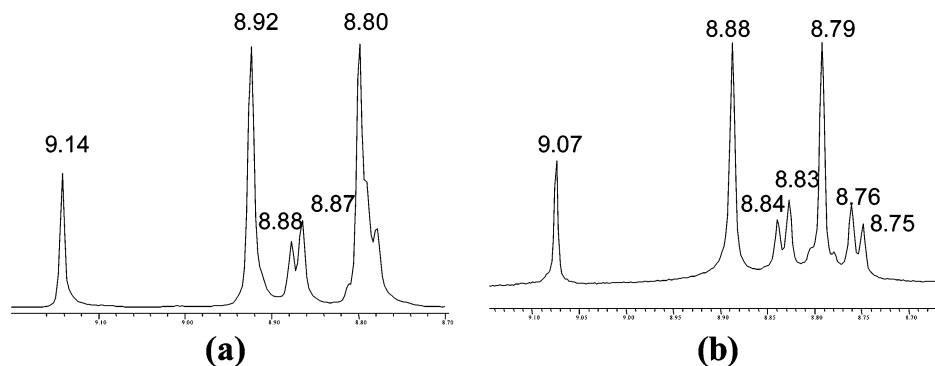
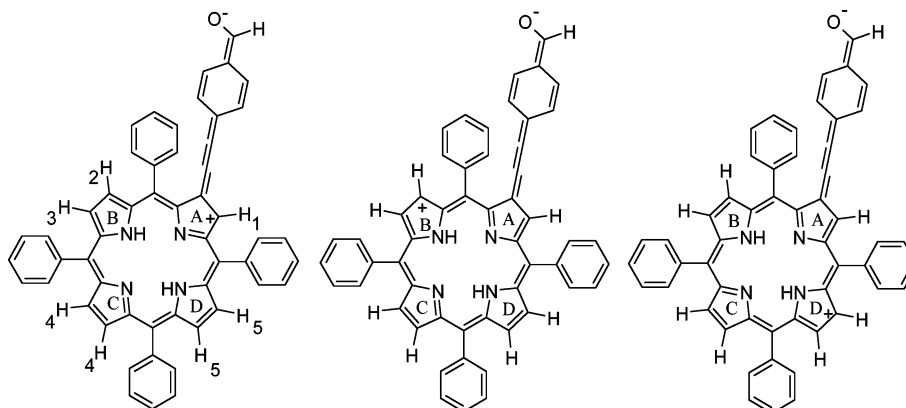**Figure 7.** ^{1}H NMR signals pattern of pyrrolic protons of (a) system A and (b) system B.

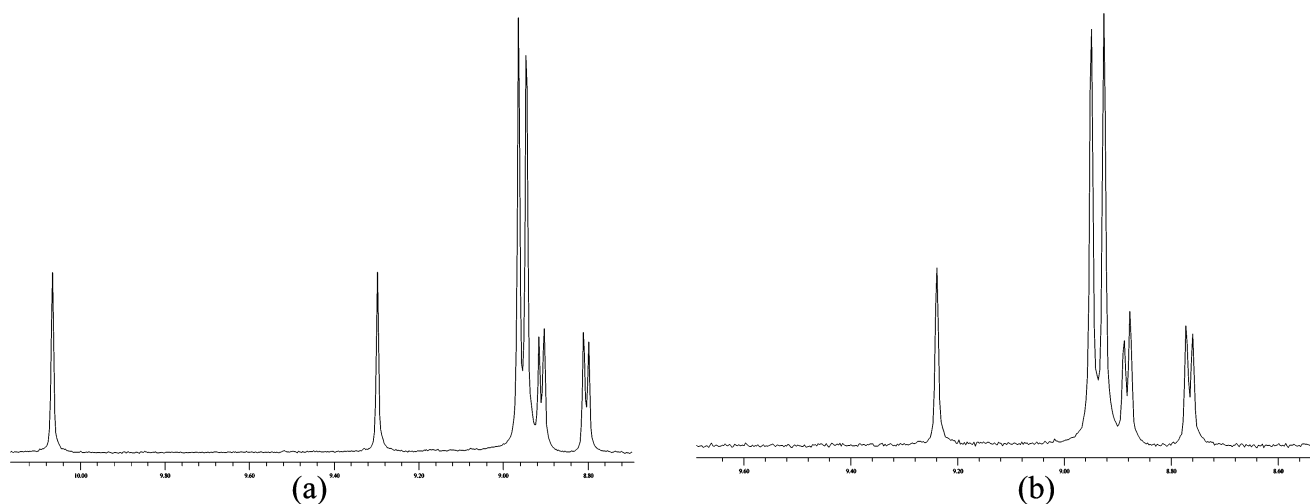
Figure 8. Three fundamental resonance structures of system A.

Figure 9. ^{1}H NMR spectra in CDCl$_3$ of Zn−system A (a) and ZnP−C$_{60}$ (b). Pyrrolic proton pattern.

zinc derivatives, the emission maxima are located at 607 and 661 nm for Zn−system A, while they are at 605 and 658 nm for Zn−system B.

Steady state fluorescence spectra of zinc derivatives in THF and benzonitrile show a substantial red shift due to the coordinating effect of the solvents. In fact, in THF, the first emission maximum of Zn−system A is at 620 nm and, in benzonitrile, it is at 628 nm.

In toluene solution, the fluorescence of the porphyrin part in H$_2$P−C$_{60}$ is quenched for 93% by the C$_{60}$ moiety. The fluorescence quenching is calculated taking system B as a reference. On the other hand, for ZnP−C$_{60}$, the quenching is 99%. In addition to the higher quenching of the porphyrin fluorescence, in the spectra of ZnP−C$_{60}$, a third emission band appears at 715 nm (Figure 10). An excitation spectrum collected

TABLE 3: Fluorescence Properties[a,b] in Different Solvents

compound	toluene			THF		
	$\lambda_{emission}$	τ	Φ	$\lambda_{emission}$	τ	Φ
system A	666	11 ns	0.11	664	11 ns	0.14
system B	663	10.9 ns	0.109	661	11.3 ns	0.138
H$_2$P−C$_{60}$[c]	663	20.5 ps	2.0×10^{-4} [c]	661	50.7 ps	6.0×10^{-4} [c]
Zn−system A	607	2.3 ns	0.05	620	2.1 ns	0.044
Zn−system B	605	2.4 ns	0.05	615	2.1 ns	0.047
ZnP−C$_{60}$	605	15.9 ps	3.5×10^{-4} [c]	615	5.8 ps	1.0×10^{-4} [c]

[a] λ_{max} in nanometers. [b] At room temperature. [c] Theoretical quantum yield related to the lifetime of the single excited state of porphyrin in the dyad.

at 715 nm (i.e., exciting from 400 to 650 nm) confirms the origin of that emission band: the porphyrin moiety. Further analysis
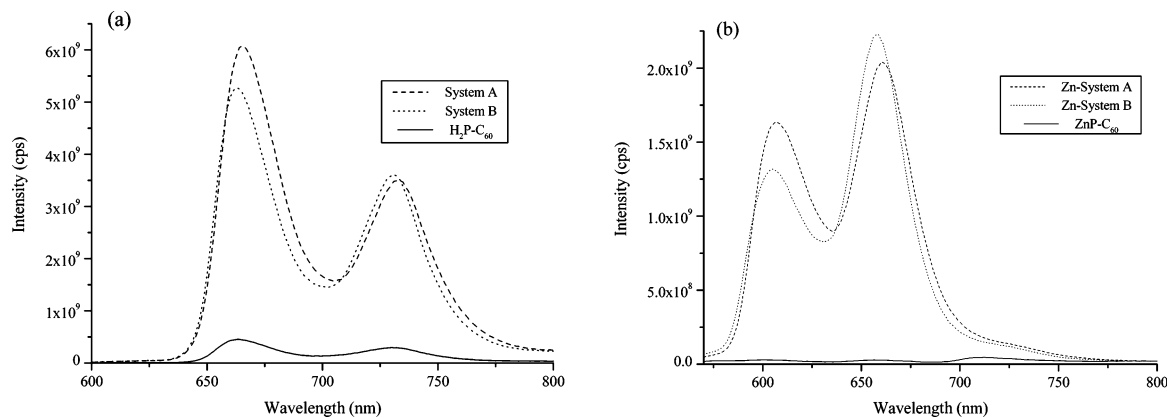
New Porphyrin Derivatives

J. Phys. Chem. A, Vol. 110, No. 40, 2006 **11431**

Figure 10. Steady state fluorescence spectra of system A, system B, and H_2P-C_{60} (a) and corresponding zinc derivatives (b) in toluene solution, respectively, upon excitation at 525 and 560 nm.
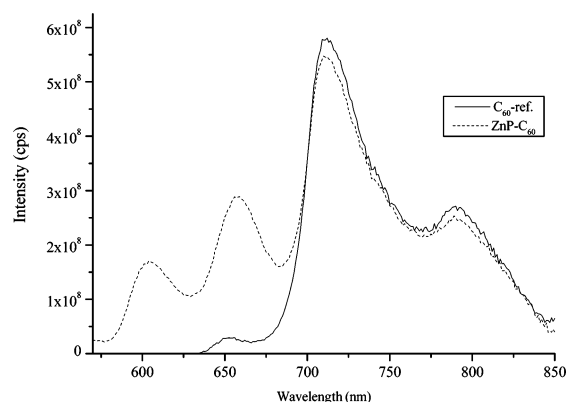

Figure 11. Steady state fluorescence spectra of C_{60}-ref and $ZnP-C_{60}$ in toluene solution upon excitation at 400 nm. The relative absorbance match (0.05 au) at excitation wavelength.

on the reference compound *N*-methyl-2-(4′-ethynyl)phenyl-3,4-fulleropyrrolidine identifies this band as the singlet excited state emission of C_{60} (Figure 11). The same behavior has also been observed in chloroform.

Such data demonstrate that in toluene solution the principal deactivation pathway of the porphyrin fluorescence is a near quantitative energy transfer from the singlet excited state of zinc porphyrin to the singlet excited state of C_{60}. In THF and benzonitrile, the porphyrin fluorescence quenching in H_2P-C_{60} is much stronger relative to what has been seen in toluene and chloroform. In $ZnP-C_{60}$ fluorescence spectra, on the other hand, we do not observe the fluorescence emission of $^{1*}C_{60}$ at 715 nm.

In general, we observe a solvent effect on the fluorescence quenching; in particular, the porphyrin fluorescence in H_2P-C_{60} tends to decrease passing from less polar to more polar solvent (Figure 12). To gather a deeper evaluation of the photophysical phenomena, time resolved fluorescence spectra were carried out in the nanosecond time domain with a 337 nm nitrogen laser.

Unfortunately, for both the free base and the zinc derivatives, the deactivation pathway of the singlet excited state of porphyrins in the dyads is faster than the time resolution. Only the C_{60} singlet excited state deactivation in the $ZnP-C_{60}$, following the energy transfer reaction in toluene, was registered.

The measured lifetime is 1.30 ± 0.01 ns, a result that is consistent with the singlet excited state lifetime of fulleropyrrolidine derivatives.[32] From the steady state fluorescence spectra of $ZnP-C_{60}$ in toluene and THF, it was possible to estimate the lifetimes of the zinc porphyrin singlet excited state. In fact,

it is possible to correlate the fluorescence quantum yield and the lifetime with the following equation:

$$\frac{\Phi_{Zn-systemB} - \Phi_{ZnP-C_{60}}}{\Phi_{ZnP-C_{60}}\tau_{Zn-systemB}} = k_{deact}$$

where $\Phi_{Zn-systemB}$ is the zinc porphyrin quantum yield, while $\Phi_{ZnP-C_{60}}$ is the zinc porphyrin quantum yield in the $ZnP-C_{60}$ and k_{deact} is the rate of the porphyrin singlet excited state deactivation process. From these analyses, we succeeded in estimating the k_{deact} value in toluene as 1.0×10^{11} s^{-1} which corresponds to a lifetime of 10 ps, while in THF a k_{deact} value of 2.0×10^{11} s^{-1} yields a lifetime of 5 ps. Such results are in agreement with the singlet excited state lifetimes measured by transient absorption spectroscopy, vide infra. Similar results were gathered for the corresponding H_2P-C_{60}.

Femtosecond transient absorption spectroscopy was used to complement the aforementioned fluorescence experiments. In particular, the references (i.e., Zn−system B and system B) and the electron donor−acceptor dyads (i.e., $ZnP-C_{60}$ and H_2P-C_{60}) were probed upon 387 nm excitation. This guarantees the predominant photoexcitation of the Zn porphyrin and free base porphyrin chromophores. At first, our attention should be directed to the references. For system B, for example, we see the nearly instantaneous formation of the singlet excited state—only a fast internal conversion (i.e., ∼2 ps) from a higher lying excited state precedes the singlet excited state formation—for which we gather the following spectral characteristics: minima at 521, 557, 600, and 660 nm and a maximum in the near-infrared at 700 nm. The minima correspond to maxima seen in the system B ground state absorption spectrum. Similar ground state bleachings (i.e., 555 and 595 nm) and new maxima in the near-infrared (i.e., 710 nm) were noted for Zn−system B. In contrast, the singlet excited state lifetimes of system B (i.e., 10.5 ns) and Zn−system B (i.e., 2.3 ns) differ fundamentally.

Mainly, the same singlet excited state formations of Zn−system B and system B were registered in $ZnP-C_{60}$ and H_2P-C_{60}, respectively, despite the presence of the electron-accepting C_{60}. This affirms in toluene and THF the successful photoexcitation of the chromophores in the electron donor−acceptor dyads. At longer delay times, however, the electron donor−acceptor dyads revealed a behavior that is vastly different from the reference systems. In particular, ultrafast deactivations of the singlet excited state are derived from kinetic analyses of the $ZnP-C_{60}$ (i.e., toluene, 15.9 ps; THF, 5.8 ps) and H_2P-C_{60} (i.e., toluene, 20.5 ps; THF, 50.7 ps) transient species in the different solvents; see Figures 13−15.

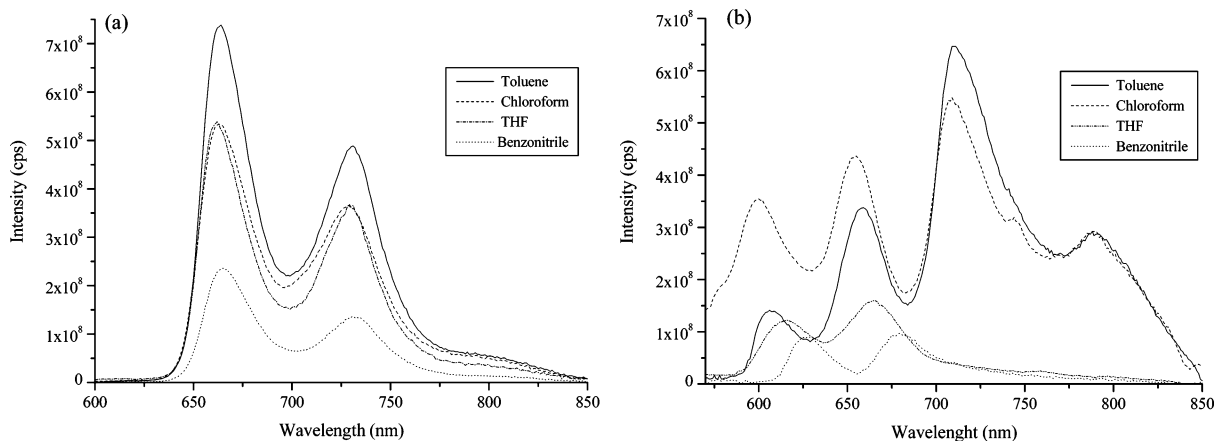**Figure 12.** Fluorescence emission spectra of H_2P-C_{60} (a) and $ZnP-C_{60}$ (b) in different solvents, respectively, upon excitation at 525 and 560 nm. The absorbance values match at excitation wavelength for both the free base and zinc derivative.
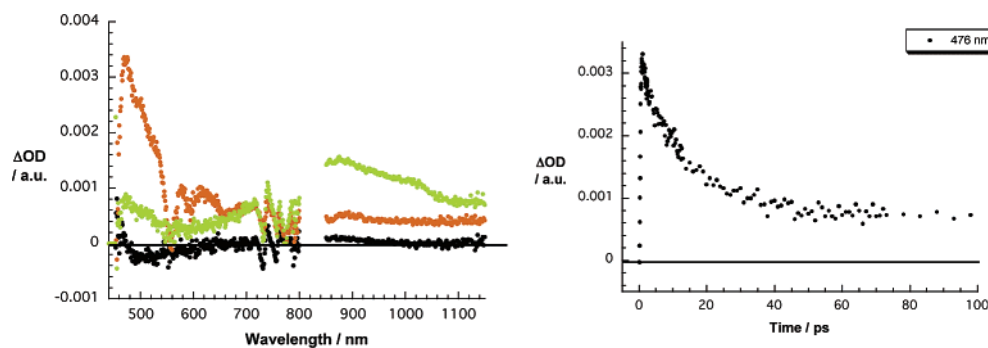

Figure 13. (left) Differential absorption spectra (visible and near-infrared) obtained upon femtosecond flash photolysis (387 nm) of $ZnP-C_{60}$ ($\sim 1.0 \times 10^{-6}$ M) in toluene with 0.05, 1.4, and 50 ps time delays at room temperature. (right) Time-absorption profile of the spectra shown above at 476 nm, reflecting the intramolecular energy transfer dynamics.
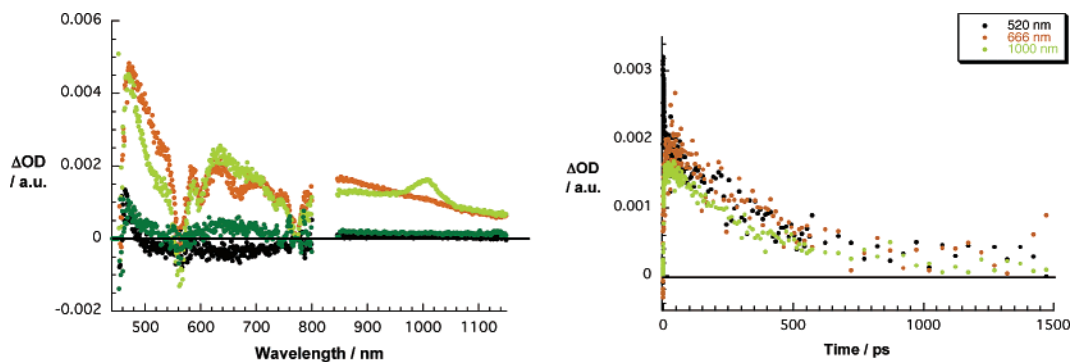

Figure 14. (left) Differential absorption spectra (visible and near-infrared) obtained upon femtosecond flash photolysis (387 nm) of $ZnP-C_{60}$ ($\sim 1.0 \times 10^{-6}$ M) in THF with 0.05, 1.4, 50, and 1525 ps time delays at room temperature. (right) Time-absorption profile of the spectra shown above at 520, 666, and 1000 nm, reflecting the intramolecular charge separation and charge recombination dynamics.

Figure 15. (left) Differential absorption spectra (visible and near-infrared) obtained upon femtosecond flash photolysis (387 nm) of H_2P-C_{60} ($\sim 1.0 \times 10^{-6}$ M) in THF with 0.05, 1.4, and 200 ps time delays at room temperature. (right) Time-absorption profile of the spectra shown above at 550, 675, and 1000 nm, reflecting the intramolecular charge separation and charge recombination dynamics.
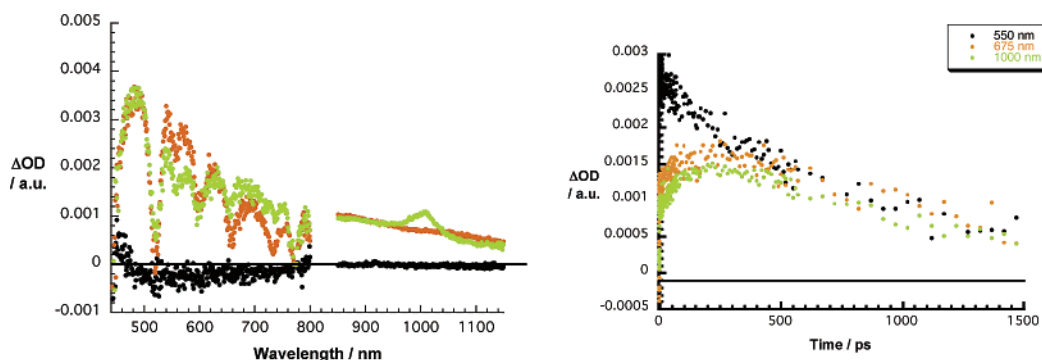
New Porphyrin Derivatives

J. Phys. Chem. A, Vol. 110, No. 40, 2006 **11433**

Spectral characteristics, which are taken immediately at the conclusion of the Zn−system B and system B singlet excited state decays, bear no resemblance with the singlet or triplet features of either chromophore. On the contrary, in toluene, the distinct absorption of the C_{60} singlet excited state evolves around 900 nm (see Figure 13), within the first 100 ps, with kinetics (i.e., ZnP−C_{60}, 17.4 ps; H_2P−C_{60}, 23 ps) that resemble the Zn−system B or system B singlet deactivations.

Therefore, we postulate that in toluene a transduction of singlet excited state energy is responsible for the kinetic and spectral observations. On the longer time scale, namely, up to 1500 ns, the C_{60} singlet/C_{60} triplet intersystem crossing takes place, which leads ultimately to the quantitative triplet formation, which is spectroscopically confirmed by the growth of a new transient that maximizes at 700 nm. In THF, on the other hand, it is not the C_{60} singlet feature in the near-infrared that is seen for both electron donor−acceptor dyads but the C_{60} radical anion bands, as gathered in Figures 14 and 15, with maxima at 1000 nm.

The C_{60} radical anion band in the near-infrared is complemented by the Zn−system B and system B radical cation absorptions in the visible with transient maxima at 635 and 690 nm, respectively. Both the radical cation and the radical anion features are formed with the same kinetics, which leads us to conclude that in THF an intramolecular electron transfer converts the initial excited state into a radical ion pair state. Moreover, the radical cation and radical anion transitions also decay with the same kinetics. From the corresponding decay dynamics, we derive lifetimes of the radical ion pair states of 398 and 1175 ps for the ZnP−C_{60} and H_2P−C_{60}, respectively. The different charge recombination dynamics (i.e., 2.5×10^9 s^{-1} versus 8.5×10^8 s^{-1}) are well in agreement with kinetics that are located in the inverted region of the parabolic dependence of electron transfer rate on the thermodynamic driving force.

Conclusions

Two new β-ethynyl porphyrins were synthesized, and the substituent effect has been studied. The new compounds show an extension of conjugation along the β-substituent, that leads to a push−pull effect when the aldehydic group is present on the phenyl ring of the substituent. These aspects are outlined by UV−vis, NMR, and cyclic voltammetry studies. Although the substituent affects the fundamental state properties of the porphyrins, it has been shown that β-substitution on the pyrrole ring deeply affects the physicochemical properties of the porphyrins, giving us a further tool to modulate porphyrin−fullerene interaction in the electron donor−acceptor systems. The new porphyrin−fullerene dyad presents a moderate charge separation state lifetime that could be improved by increasing the porphyrin−fullerene distance. This prompts us to study the "photonic wire" behavior of an enlarged spacer.

Supporting Information Available: HSQC and HMBC NMR spectra of systems A and B; drawings of the theoretical resonance structures of system A; a comparison between the UV−vis spectra of H_2−TPP, system A, and system B; and cyclic voltammograms of H_2−TPP, system A, and system B in DCB. This material is available free of charge via the Internet at http://pubs.acs.org.

References and Notes

(1) Guldi, D. M. *Chem. Soc. Rev.* **2002**, *31*, 22−36.

(2) (a) Ben-Shem, A.; Frolow, F.; Nelson, N. *Nature* **2003**, *426*, 630−635. (b) Hasegawa, J.; Ohkawa, K.; Nakatsuji, H. *J. Phys. Chem. B* **1998**, *102*, 10410−10419. (c) Hasegawa, J.; Nakatsuji, H. *J. Phys. Chem. B* **1998**, *102*, 10420−10430. (d) Kirmaier, C.; Bautista, J. A.; Laible, P. D.; Hanson, D. K.; Holten, D. *J. Phys. Chem. B* **2005**, *109*, 24160−24172. (e) Ivashin, N.; Larsson, S. *J. Phys. Chem. B* **2005**, *109*, 23051−23060. (f) Ziolek, M.; Pawlowicz, N.; Naskrecki, R.; Dobek, A. *J. Phys. Chem. B* **2005**, *109*, 18171−18176

(3) (a) Ikeda, A.; Hatano, T.; Shinkaj, S.; Akijama, T.; Yamada, S. *J. Am. Chem. Soc.* **2001**, *123*, 4855−4856. (b) Imahori, H.; Norieda, H.; Yamada, H.; Nishimura, Y.; Yamazaki, I.; Sakata, Y.; Fukuzumi, S. *J. Am. Chem. Soc.* **2001**, *123*, 100−110. (c) Hasabe, T.; Imahori, H.; Kamat, P. V.; Ahu, T. K.; Kim, S. K.; Kim, S.; Fujimoto, A.; Hirokawa, T.; Fukuzumi, S. *J. Am. Chem. Soc.* **2005**, *127*, 1216−1228.

(4) (a) D'Souza, F.; Daviprasad, G. R.; Zandler, M. E.; Hoang, V. T.; Klykov, A.; Van Stipdaik, M.; Perera, A.; El-Khouly, M. E.; Fujitsuka, M.; Ito, O. *J. Phys. Chem. A* **2002**, *106*, 3243−3252. (b) Satake, A.; Kobuke, Y. *Tetrahedron* **2005**, *61*, 13−41. (c) Da Ros, T.; Prato, M.; Carano, M.; Ceroni, P.; Paolucci, F.; Roffia, S.; Valli, L.; Guldi, D. M. *J. Organomet. Chem.* **2000**, *599*, 62−68. (d) D'Souza, F.; Deviprasad, G. R.; Zandler, M. E.; El-Khouly, M. E.; Fujitsuka, M.; Ito, O. *J. Phys. Chem. A* **2003**, *107*, 4801−4807. (e) Balbinot, D.; Atalick, S.; Guldi, D. M.; Hatzimarinaki, M.; Hirsch, A.; Jux, N. *J. Phys. Chem. B* **2003**, *107*, 13273−13279. (f) Boyd, P. D. W.; Reed, C. A. *Acc. Chem. Res.* **2005**, *38*, 235−242.

(5) (a) Imahori, H.; Tamaki, K.; Guldi, D. M.; Luo, C.; Fujitsuka, M.; Ito, O.; Sakata, Y.; Fukuzumi, S. *J. Am. Chem. Soc.* **2001**, *123*, 2607−2617. (b) Kodis, G.; Liddell, P. A.; de la Garza, L.; Clausen, P. C.; Lindsey, J. S.; Moore, A. L.; Moore, T. A.; Gust, D. *J. Phys. Chem. A* **2002**, *106*, 2036−2048.

(6) Gust, D.; Moore, T. A.; Moore, A. L. *Acc. Chem. Res.* **1993**, *26*, 198−205.

(7) Imahori, H.; Sekiguchi, Y.; Kashiwagi, Y.; Sato, T.; Araki.; Y.; Ito, O.; Yamada, H.; Fukuzumi, S. *Chem.−Eur. J.* **2004**, *10*, 3184−3196.

(8) Imahori, H.; Yamada, H.; Nishimura, Y.; Yamazaki, I.; Sakata, Y. *J. Phys. Chem. B* **2000**, *104*, 2099−2108.

(9) Guldi, D. M.; Imahori, H.; Tamaki, K.; Kashiwagi, Y.; Yamada, H.; Sakata, Y.; Fukuzumi, S. *J. Phys. Chem. A* **2004**, *108*, 541−548.

(10) Imahori, H.; Guldi, D. M.; Tamaki, K.; Yoshida, Y.; Luo, C.; Sakata, Y.; Fukuzumi, S. *J. Am. Chem. Soc.* **2001**, *123*, 6617−6628.

(11) Choi, M. S.; Yamazaki, T.; Yamazaki, I.; Aida, T. *Angew. Chem., Int. Ed.* **2004**, *43*, 150−158.

(12) (a) Imahori, H. *J. Phys. Chem. B* **2004**, *108*, 6130−6143. (b) Gould, S. L.; Kodis, G.; Palacios, R. E.; De la Garza, L.; Brune, A.; Gust, D.; Moore, T. A.; Moore, A. L. *J. Phys. Chem. B* **2004**, *108*, 10566−10580.

(13) Drovetskaya, T.; Reed, C. A.; Boyd, P. D. W. *Tetrahedron Lett.* **1995**, *36*, 7971−7974.

(14) Kuciauskas, D.; Liu, S.; Seely, G. R.; Moore, A. L.; Moore, T. A.; Gust, D.; Drovetskaya, T.; Reed, C. A.; Boyd, P. D. W. *J. Phys. Chem.* **1996**, *100*, 15926−15932.

(15) Okhubo, K.; Imahori, H.; Shao, J.; Ou, Z.; Kadish, K. M.; Chen, Y.; Zheng, G.; Pandey, R. K.; Fujitsuka, M.; Ito, O.; Fukuzumi, S. *J. Phys. Chem. A* **2002**, *106*, 10991−10998.

(16) Okhubo, K.; Kotani, H.; Shao, J.; Ou, Z.; Kadish, K. M.; Li, G.; Pandey, R. K.; Fujitsuka, M.; Ito, O.; Imahori, H.; Fukuzumi, S. *Angew. Chem., Int. Ed.* **2004**, *43*, 853−856.

(17) (a) Guldi, D. M.; Nuber, B.; Bracher, P. J.; Alabi, C. A.; MacMahon, S.; Kukol, J. W.; Wilson, S. R.; Schuster, D. I. *J. Phys. Chem. A* **2003**, *107*, 3215−3221. (b) Kashiwagi, Y.; Ohkubo, K.; McDonald, J. A.; Blake, I. M.; Crossley, M. J.; Araki, Y.; Ito, O.; Imahori, H.; Fukuzumi, S. *Org. Lett.* **2003**, *5*, 2719−2721

(18) Meier, H.; Mühling, B.; Kolshorn, H. *Eur. J. Org. Chem.* **2004**, 1033−1042.

(19) Fau, F. R. F.; Lai, R. Y.; Cornil, J.; Karzaki, Y.; Bredas, J. L.; Cai, L.; Cheng, L.; Yao, Y.; Price, D. W., Jr.; Dirk, S. M.; Tour, J. M.; Bard, A. J. *J. Am. Chem. Soc.* **2004**, *126*, 2568−2573.

(20) Yeung, M.; Ng, A. C. H.; Drew, M. G. B.; Vorpagel, E.; Breitung, E. M.; McMahon, R. J.; Ng, D. K. P. *J. Org. Chem.* **1998**, *63*, 7143−7150.

(21) (a) Thorand, S.; Krause, N. *J. Org. Chem.* **1998**, *63*, 8551−8553. (b) Austin, W. B.; Bilow, N.; Kelleghan, W. J.; Lau, K. S. J. *J. Org. Chem.* **1981**, *46*, 2280−2286.

(22) Callot, H. J. *Bull. Soc. Chim. Fr.* **1974**, *7−8*, 1492−1496.

Lembo et al.

(23) (a) Lindsey, J. S.; Prataphan, S.; Johnson, T. E.; Wagner, R. W.; *Tetrahedron* **1994**, *50* (30), 8941−8968. (b) Wagner, R. W.; Johnson, T. E.; Lindsey, J. S. *J. Am. Chem. Soc.* **1996**, *118*, 11166−11180. (c) Wagner, R. W.; Johnson, T. E.; Li, F.; Lindsey, J. S. *J. Org. Chem.* **1995**, *60*, 5266−5273.

(24) (a) Maggini, M.; Scorrano, G. *J. Am. Chem. Soc.* **1993**, *115*, 9798−9799. (b) Zilbermann, I.; Anderson, G. A.; Guldi, D. M.; Yamada, H.; Imahori, H.; Fukuzumi, S. *J. Porphyrins Phthalocyanines* **2003**, *7*, 357−364.

(25) (a) Cyclic voltammetry measurements of H₂TPP, system A, and system B were reported in the Supporting Information. (b) Kadish, K. M.; Lindsey, J. S. *Handbook of Porphyrins and Phthalocyanine*; Kadish, K. M., Guilard, R., Smith, K. M., Eds.; Vol. 9. (c) Autret, M.; Ou, Z.; Antonini, A.; Boschi, T.; Tagliatesta, P.; Kadish, K. M. *J. Chem. Soc., Dalton Trans.* **1996** 2793−2797. (d) Kadish, K. M.; Guo, N.; Van Caemelbecke, E.; Froiio, A.; Paolesse, R.; Monti, D.; Tagliatesa, P.; Boschi, T.; Prodi, L.; Bolletta, F.; Zaccheroni, N. *Inorg. Chem.* **1998**, *37* (10), 2358−2365.

(26) (a) D'Souza, F.; Zandler, M. E.; Tagliatesta, P.; Ou, Z.; Shao, J.; Van Caemelbecke, E.; Kadish, K. M. *Inorg. Chem.* **1998**, *37*, 4567−4572. (b) Kadish, K. M.; D'Souza, F.; Villard, A.; Autret, M.; Van Caemelbecke, E.; Blanco, P.; Antonini, A.; Tagliatesta, P. *Inorg. Chem.* **1994**, *33*, 5169−5170. (c) Binstead, R. A.; Crossley, M. J.; Hush, N. J. *Inorg. Chem.* **1991**, *30*, 1259−1264.

(27) Comparisons between the UV−vis spectrum of TPP and the UV−vis spectra of both of the new synthesized porphyrins in toluene solution are reported in the Supporting Information.

(28) (a) Bax, A.; Summers, M. F. *J. Am. Chem. Soc.* **1986**, *108*, 2093−2094. (b) Bax, A.; Marzilli, L. G.; Summers, M. F. *J. Am. Chem. Soc.* **1986**, *108*, 4285−4294.

(29) All of the heteronuclear ¹H−¹³C NMR spectra are reported in the Supporting Information.

(30) The three depicted resonance structures are those significative to explain the magnetical differences occurring in the proton and carbon signals of the β-pyrrolic positions. In fact, there are many different resonance structures induced by the β-substituent, as it's possible to see in the Supporting Information.

(31) Crossley, M.; Harding, M. M.; Sternell, S. *J. Am. Chem. Soc.* **1986**, *108*, 3608−3613.

(32) Guldi, D. M.; Prato, M. *Acc. Chem. Res.* **2000**, *33*, 695−703.